Thin-Film Silicon Solar Cells on 1-D Periodic Gratings With Nonconformal Layers: Optical Analysis

Article *in* IEEE Journal of Photovoltaics · January 2013

DOI: 10.1109/JPHOTOV.2012.2220123

4 authors:

Serge Solntsev
Delft University of Technology
20 PUBLICATIONS **312** CITATIONS
SEE PROFILE

Olindo Isabella
Delft University of Technology
153 PUBLICATIONS **1,510** CITATIONS
SEE PROFILE

Diego Caratelli
142 PUBLICATIONS **947** CITATIONS
SEE PROFILE

Miro Zeman
Delft University of Technology
442 PUBLICATIONS **6,552** CITATIONS
SEE PROFILE

Thin-Film Silicon Solar Cells on 1-D Periodic Gratings With Nonconformal Layers: Optical Analysis

Serge Solntsev, Olindo Isabella, Diego Caratelli, and Miro Zeman

***Abstract*—Design of 1-D submicrometer periodic gratings aimed at the enhancement of the short-circuit current density in thin-film silicon solar cells is investigated. A rigorous full-wave analysis is carried out to determine the absorption in amorphous (a-Si:H) and microcrystalline (μc-Si:H) silicon solar cells on substrates with gratings featuring different geometrical characteristics. Maximal photocurrent densities $J_{\rm ph}$ are evaluated in both superstrate (p-i-n) and substrate (n-i-p) configurations, taking into account the nonconformal growth of the layers on the gratings. The $J_{\rm ph}$ relative to that of corresponding flat solar cells was found to be 1.34, 1.24, 1.23, and 1.38 times higher for p-i-n a-Si:H, μc-Si:H-based structures, and n-i-p a-Si:H, μc-Si:H based structures, respectively.**

***Index Terms*—Light trapping, photovoltaic cell, semiconductor device modeling, silicon.**

I. Introduction

IN THIN-FILM silicon solar cells, different light trapping methods are used to maximize the absorption in the active layer in order to increase energy conversion efficiency. Random texturing of the surface of solar cell substrates is a commonly used technique [1]–[3] to enhance scattering inside solar cells. Submicrometer periodic gratings (SPGs) [4], [5] represent an alternative design solution to randomly surface-textured morphologies. Although theoretical analysis shows that 2-D grating structures feature a superior performance compared with devices based on 1-D gratings [6]–[8], the symmetry of the latter structure can be used to reduce the model complexity while still considering all wave effects. Results reported in [9]–[12] demonstrate that applying SPG in solar cells can result in photocurrents comparable with those with randomly surface-textured substrates. However, the optimization of geometry of the SPG is needed to further increase the energy conversion efficiency [13], [14]. In order to determine the complex light intensity distribution in grating-textured solar cells, various computational electromagnetic techniques have been used [15]–[20]. Recently, we have studied light trapping in thin-film silicon solar cells for light in the wavelength range from 660 to 1000 nm [21], [22]. In this paper, the analysis of light behavior in thin-film silicon solar cells is extended to a wider wavelength region, from 350 to 1000 nm. This allows us to investigate both light trapping and the antireflective effect due to the application of periodic textures in the solar cells. The numerical solution of Maxwell equations in realistic amorphous and microcrystalline silicon (a-Si:H and μc-Si:H) solar cells on SPG in both superstrate and substrate configurations has been carried out by using the finite-difference time-domain (FDTD) method [23]. In particular, the software package MEEP [24] has been used for the numerical implementation of the FDTD electromagnetic solver. Furthermore, a dedicated MATLAB [25]-based modeling tool has been developed to handle the numerical simulations and postprocess the results. The total reflectance and transmittance of the solar cell and the absorption level in the individual layers have been accurately evaluated as a function of the wavelength. The optical dispersion of the layers in the solar cells has been described by using wavelength-dependent permittivity functions. Since the solver requires a Lorentzian-like harmonic series representation of the dielectric constant of the dispersive materials, a numerical fitting procedure has been developed for an accurate modeling of these physical phenomena. The nonconformal growth of the layers on SPG has been taken into account in the simulations. Since the morphology of the interfaces in the solar cell changes from layer to layer [26], this aspect has to be carefully addressed in order to analyze the impact of the nonconformal growth in the solar cell structure with rough interfaces on the light trapping properties. We have therefore demonstrated that the morphology of the consecutive interfaces has a significant impact on the absorption level in thin-film silicon solar cells.

II. Simulation Details

A. Description of the Optical Model

The electric field distribution within a solar cell structure is determined by solving Maxwell's equations governing the propagation, reflection, and diffraction of electromagnetic waves. To this end, MEEP routines [24], which are based on the FDTD method, have been used in this study. In the FDTD method, the 3-D space is divided into a discrete grid and the electromagnetic field is evolved in time by using a discrete marching-in-time scheme. Applying the Fourier transformation to the response of the structure to an excitation pulse, the entire frequency

Manuscript received June 7, 2012; revised August 3, 2012 and September 14, 2012; accepted September 14, 2012. This work was supported by the Dutch Ministry of Economic Affairs in the framework of "Cheoptics" project.

S. Solntsev, O. Isabella, and M. Zeman are with the Photovoltaic Materials and Devices Group/Delft Institute of Microsystems and Nanoelectronics, Delft University of Technology, 2628CD Delft, The Netherlands (e-mail: s.solntsev@tudelft.nl; o.isabella@tudelft.nl; m.zeman@tudelft.nl).

D. Caratelli is with the International Research Centre for Telecommunications and Radar, Delft University of Technology, 2628CD Delft, The Netherlands (e-mail: D.Caratelli@tudelft.nl).

Color versions of one or more of the figures in this paper are available online at http://ieeexplore.ieee.org.

Digital Object Identifier 10.1109/JPHOTOV.2012.2220123

spectrum of the parameters of interest is obtained in a single-run simulation. The solver supports three basic types of boundary conditions: the Bloch-periodic boundaries, the metallic walls, and the perfectly matched layers (PMLs). Symmetry of the structure can be used to reduce the size of the unit cell.

The physical properties of the materials in Maxwell's equations are described in terms of electric permittivity and magnetic permeability, which are position- and frequency-dependent. In the developed model, the material dispersion is described by means of Lorentzian-like harmonic series extended with a frequency-independent term, accounting for the electrical conductivity of the medium. Therefore, experimentally measured permittivity and permeability functions have to be represented analytically in the aforementioned form using a suitable fitting procedure. An inaccurate fit of material properties results in (over-) under-estimation of the electric field distribution. To minimize these errors, a dedicated local fitting approach, which is described in the next section, has been adopted.

To analyze the response of the solar cell to both polarizations, the structure has been excited by plane wave propagating in the direction normal to the top dielectric interface. The source pulse has equal p- and s-polarization components and Gaussian temporal dependence with central frequency and width set in such a way that the pulse energy is mainly confined in the wavelength range of interest. It has been found that for the considered class of devices, the adoption of a uniform computational mesh with grid size of 3.3 nm allows us to keep the numerical error below 2% (the grid size was tested down to 0.8 nm). Therefore, a simulation domain size of $\sim$10 μm^2 results in about 0.9 $\times$ 10^6 grid points. Typical simulation time was from 4 to 7 h for each run with a memory usage level of about 1 GB on a workstation equipped with two 4-core processors. In all numerical simulations, a Courant factor equal to 0.5 has been selected. The performed computations were stopped as soon as the ratio between the intensity of the electric field in the simulation domain and the relevant peak value was found to be 10^{-6}. Total reflectance and transmittance of the structure have been evaluated, and electric field spatial distribution $E(r, \lambda)$ as a function of wavelength λ has been computed. The absorption level $A_i(\lambda)$ of the ith layer in the solar cell is computed by integrating $E(r, \lambda)$ (divided by electric field distribution for the case without the structure $E_0(r, \lambda)$) inside its volume V_i

$$A_i(\lambda) = k(\lambda)\mathrm{Im}\left[\varepsilon_i(\lambda)\right] \int_{V_i} \frac{|E(r,\lambda)|^2}{|E_0(r,\lambda)|^2} dV \tag{1}$$

where $k(\lambda)$ is a scaling coefficient, $\varepsilon_i(\lambda)$ denotes the relative permittivity of the ith layer, and r is the position vector within the structure. The scaling of $A_i(\lambda)$ is necessary because in MEEP, the excitation of the electromagnetic field within the structure under analysis is carried out by using *current* sources, but no relation can be established *a priori* between the *current* source and the resulting field amplitudes; such a relation strongly depends on the geometrical, as well as electrical, properties of the device. As it is difficult to calculate the incident flux induced by such sources, a way to evaluate the absorption level is to enforce the energy conservation principle $R(\lambda) + \sum_i A_i(\lambda) + T(\lambda) = 1$. The absorption in the individual layers can be expressed in terms of the photocurrent density $J_{i\text{-ph}}$ by integrating the absorption level $A_i(\lambda)$ with the AM1.5G spectrum [27] $S(\lambda)$ in the wavelength range of interest (350–1000 nm)

$$J_{i\text{-ph}} = \frac{q}{hc} \int_{\lambda_{\min}}^{\lambda_{\max}} \lambda \cdot A_i(\lambda) \cdot S(\lambda) d\lambda \tag{2}$$

where q is the elementary charge, h is Planck's constant, and c is the speed of light. Here, it is assumed that each absorbed photon generates one electron–hole pair and that all photogenerated carriers are collected.

B. Fitting the Material Optical Properties

For a reliable evaluation of the absorption in each individual layer of the solar cell, an analytical representation of the optical properties of the dispersive materials in the solar cell has to be used in the MEEP calculations. Therefore, an accurate matching between the simulated and experimental values of the permittivity and magnetic permeability of each material is needed.

As the materials used in the thin-film silicon solar cells are nonmagnetic, their relative magnetic permeability is set to unity. On the other hand, the electric permittivity of the transparent conductive oxides (TCOs), silicon-based layers, and silver strongly depends on wavelength (optical dispersion). This requires the fitting of the measured properties of the layers by means of harmonic series expansions. We have found that describing the permittivity of layers in the whole wavelength range of interest (350–1000 nm) with only one set of parameters typically results in a large inaccuracy. For example, in the case of a-Si:H for wavelengths longer than 650 nm, a relative error larger than 200% in the imaginary part of the permittivity has been observed. Such errors result in an overestimation of the absorption level. In order to tackle this problem, the wavelength spectrum was split up into three regions: "short" (350–550 nm), "medium," (550–660 nm), and "long" (660–1000 nm); details are given in [22].

C. Comparison With Other Simulators

A comparison of the MEEP modeling tool with other electromagnetic field solvers, such as Computer Simulation Technology Microwave Studio (CST) [28], Ansys High-Frequency Structure Simulator (HFSS) [29], and Advanced Semiconductor Analysis (ASA) [30], was carried out for a flat a-Si:H p-i-n solar cell. In particular, we have designed a multilayered structure on semi-infinite glass (incident medium) with flat interfaces, consisting of a 0.6-μm-thick aluminum-doped zinc-oxide (ZnO:Al) layer as a front TCO, a 0.3-μm a-Si:H slab as an absorber layer, a 0.1-μm-thick ZnO:Al layer as a back TCO, and a 0.3-μm-thick Ag layer as a back reflector. In order to further assess the accuracy of the developed FDTD-based procedure, a test case involving gratings has also been considered. In particular, a structure consisting of glass substrate with a semicircular grating having period 1 μm, radius 0.25 μm, covered by 0.15-μm-thick a-Si:H layer has been analyzed. It has been found out

TABLE I
STATISTICS OF DIFFERENCES IN a-Si:H ABSORPTION LEVELS BETWEEN THE RESULTS OF MEEP AND THE OTHER SOLVERS IN WAVELENGTH RANGE 350–1000 nm

Test structure	MEEP results compared with	Mean difference	Standard deviation of difference
Flat pin structure	ASA	0.0001	0.0333
	CST	0.0046	0.0333
	HFSS	0.0004	0.0337
1-D SPG with a-Si:H layer	HFSS	-0.0023	0.0124

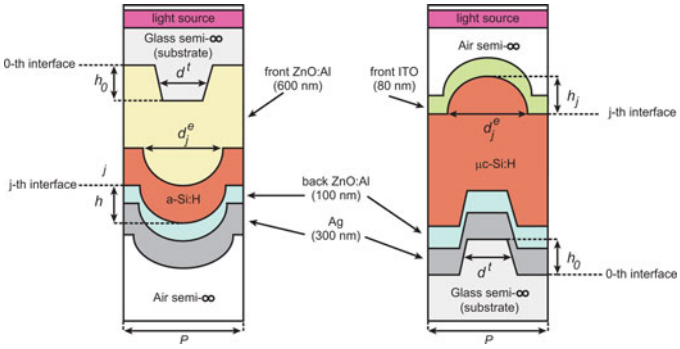

Fig. 1. Selected geometries of the simulated structures. (Left) a-Si:H p-i-n and (right) μc-Si:H n-i-p. PML layers are not shown.

that the numerical results obtained by using MEEP and the other solvers are in close agreement, as shown in Table I.

D. Simulated Solar Cell Structures

Both superstrate (p-i-n) and substrate (n-i-p) configurations of single-junction thin-film silicon solar cells using a-Si:H and μc-Si:H absorber layers have been investigated. The main difference between the two configurations lies in the deposition sequence of the p-i-n junction, which influences the interface morphology between the layers, as well as the thickness and composition of the front TCO.

The simulated p-i-n configuration is shown in Fig. 1(left). It consists of top semi-infinite patterned glass, aluminum-doped zinc-oxide (ZnO:Al, 0.6 μm thick) as front TCO, a-Si:H or μc-Si:H as absorber layer, a combination of back ZnO:Al (0.1 μm) and Ag (0.3 μm) as back reflector, and a semi-infinite air layer. The simulated n-i-p configuration is the reverse of the p-i-n configuration [see Fig. 1(right)]. From bottom to top, a semi-infinite patterned glass serves as the substrate for back reflector (Ag and back ZnO:Al), back ZnO:Al (0.1 μm), a-Si:H or μc-Si:H constitutes the absorber layer, a film of indium tin oxide (ITO) (0.1/0.08 μm a-Si:H/μc-Si:H) is the front TCO, and a semi-infinite air layer ends the structure.

The source of electromagnetic radiation was placed inside the glass layer in the case of the p-i-n structure and inside the air layer above the ITO in the case of the n-i-p structure. The incident media were modeled as semi-infinite dielectric slabs by applying PML boundary condition to their outer sides. Periodic boundary condition was used along the side walls of the solar

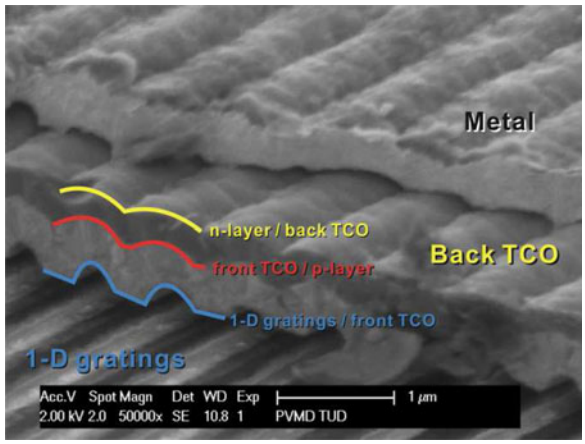

Fig. 2. Cross-sectional SEM image of a typical p-i-n single-junction a-Si:H solar cell on 1-D SPG.

cell structure. The complexity of the simulated structures was reduced to two dimensions by taking advantage of the symmetry of the structure with 1-D SPG. In the case of p-i-n devices, the reflection from the air/glass interface was neglected in the direct FDTD-based simulations with the light source located inside the glass layer. This additional reflection has been properly taken into account in the postprocessing of the simulation results by using the classical infinite sum formula.

Surface morphology measurements of solar cell structures showed the nonconformal growth of a thick ZnO:Al or μc-Si:H on the trapezoidal SPG. Due to this effect, both the peak-to-peak height and duty cycle of the SPG change from layer to layer; see Fig. 2 for an example.

E. Modeling Texture Development

Modeling of the solar cell structure requires special attention because in the case of nonconformal growth, the grating morphology is different for each interface. In both the p-i-n and n-i-p cases, the substrate engraved with 1-D SPG has been labeled as the 0th layer. The duty cycle d_{C0} at the 0th interface was defined as d^t/P, where d^t is the width of the trapezoid at half height $(h_0/2)$ (see Fig. 1). For the next interface, we assume that this trapezoid is smoothened and transformed into an ellipse. This smoothening continues for all subsequent interfaces, which reduces the height and increases the width of the ellipse by a factor LVL

$$\begin{cases} h_1 = \dfrac{h_0}{\mathrm{LVL}_1} \\ d_1^e = d^t \cdot \mathrm{LVL}_1 \end{cases} \Rightarrow \begin{cases} h_j = \dfrac{h_{j-1}}{\mathrm{LVL}_j} \\ d_j^e = d_{j-1}^e \cdot \mathrm{LVL}_j . \end{cases}$$

Here, LVL_j is the degree of leveling of interface j and calculated using

$$\mathrm{LVL}_j = L + (L-1) \cdot t_i \tag{3}$$

where t_i is the thickness of the ith layer, and parameter L, which is the same for all layers, describes the different growth mechanisms from purely conformal ($L = 1$) to isotropic growth ($L = 1.5$). In case growth is conformal, LVL_j is independent

TABLE II
SIMULATION PARAMETER SPACE

parameter	min	step	max
P [µm]	0.25	0.25	1.0
h [µm]	0.05	0.10	0.55
L [-]	1.0	0.1	1.5
$t_{a\text{-}Si:H}$ [µm]	0.1	0.1	0.3
$t_{\mu c\text{-}Si:H}$ [µm]	0.5	0.5	2.0

from the thickness ($\mathrm{LVL}_j = L = 1$), while for isotropic growth, the parameter L controls how quickly the initial morphology tends to be flattened after a certain thickness. We found that $L = 1.5$ is already an extreme value for quickly flattening an interface.

The parameter space that is investigated with our simulations is shown in Table II, where the sweeping ranges for P, h_0, L, and p-i-n, n-i-p cells absorber thickness (t) are reported. Parameter d_{C0} was kept constant to 0.5, and other properties and sizes of the structures were kept the same throughout the simulations.

III. RESULTS OF SIMULATIONS

In this section, the optical modeling of a-Si:H and μc-Si:H solar cells on SPG in both p-i-n and n-i-p configurations is discussed in detail. Our aim was to maximize the absorption level in the silicon-based layers of the investigated solar cells. As a reference, we have calculated the absorptions of 0.3-μm-thick a-Si:H and of 1-μm-thick μc-Si:H absorbers in solar cell structures with flat interfaces and expressed them in a photocurrent density $J_{\mathrm{ph\text{-}flat}}$, according to (2). In this study, we did not model the doped layers included in the solar cell structures. As outlined in previous studies [20], the change in grating period and height has little effect on the absorption level in p- and n-layers. That is why the modeling of the aforementioned layers has been neglected in the current study, therefore achieving a favorable effect on the calculation times. While changing the structure parameters, we assumed that the overestimation of J_{ph} remains constant, and therefore, the simulations still give correct optimal values for particular solar cell structures. The ratio $J_{\mathrm{ph}}/J_{\mathrm{ph\text{-}flat}}$ has been used as an indicator of the enhanced absorption in solar cell structures on SPG with respect to the flat structures. We present the optimal parameters P, h, and L of the SPG resulting in the maximum enhancement of the J_{ph}. Subsequently, we investigate the impact of the thickness t of the silicon absorber layers (a-Si:H and μc-Si:H) in p-i-n configuration on the optimal values of P and h. Next, we analyze the antireflection (AR) effect of SPG in the "short" and "medium" wavelength ranges, as well as the light trapping properties in the "long" wavelength range for a-Si:H and μc-Si:H solar cells in both p-i-n and n-i-p configurations.

A. a-Si:H p-i-n Solar Cells

The thickness of the a-Si:H absorber in the p-i-n solar cell was fixed to 0.3 μm. The period, height, and leveling were varied according to Table II. Maximal J_{ph} (15.5 mA/cm^2) was achieved by selecting the grating parameters $P = 0.75$ μm, $h = 0.45$ μm, and $L = 1.3$ (see Fig. 3). For conformal growth ($L = 1$), maximal $J_{\mathrm{ph}} = 15$ mA/cm^2 corresponds to $P = 0.25$ μm. It was found that structures with a smaller P exhibit an increased absorption level in a-Si:H absorber in the "short" wavelength range, whereas the absorption reduces at wavelengths larger than 600 nm. On the other hand, solar cell structures with larger P exhibit a larger absorption at "long" wavelengths due to enhanced scattering. At "short" wavelengths, the absorption in solar cell structures with larger P decreases because of the higher total reflection. Losses in the front TCO in the a-Si:H p-i-n structures are considerable, as shown in Fig. 4.

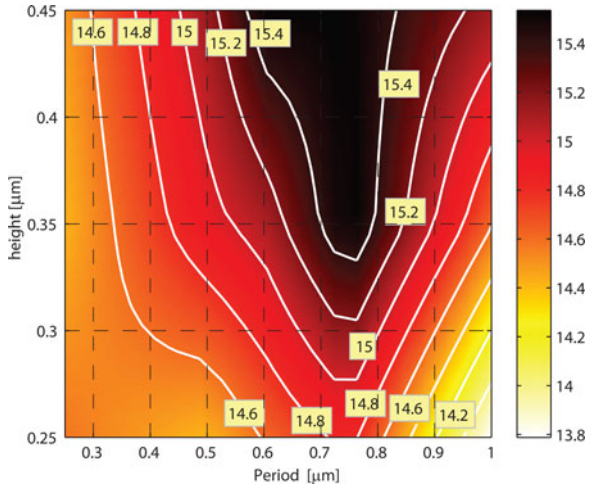

Fig. 3. J_{ph} [mA/cm^2] of a-Si:H p-i-n solar cell with absorber thickness 0.3 μm, $L = 1.3$ as a function of period P and height h of the periodic gratings.

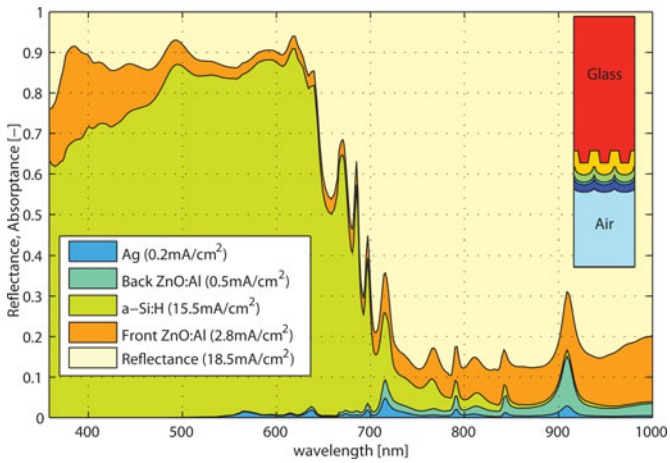

Fig. 4. Absorption of the layers and total reflectance of the a-Si:H p-i-n solar cell with absorber thickness 0.3 μm as a function of wavelength for $P = 0.75$ μm, $h = 0.45$ μm, and $L = 1.3$.

B. µc-Si:H p-i-n Solar Cells

The thickness of the μc-Si:H absorber in the p-i-n solar cells has been fixed to 1.0 μm. Maximal J_{ph} (20.3 mA/cm^2) has been obtained for $P = 0.50$ μm, $h = 0.45$ μm, and $L = 1.3$. The same solar cell structure, with $P = 0.75$ μm, has resulted in a similar J_{ph} of 20.1 mA/cm^2. Similar to the structures with an a-Si:H

absorber, a smaller P leads to a higher absorption in the μc-Si:H absorber in the "short" wavelength range due to a prominent AR effect occurring at the glass/TCO and TCO/Si:H interfaces. The structures with a larger P feature larger absorption in the "long" wavelength range due to enhanced scattering. Losses (including the total reflectance) have been found to be lower than in the case of a-Si:H p-i-n solar cells with the same combinations of grating parameters.

C. a-Si:H n-i-p Solar Cells

In n-i-p solar cell, the thickness of the a-Si:H absorber has been fixed to 0.3 μm. Maximal $J_{\rm ph}$ (16.4 mA/cm^2) has been achieved for the set of parameters $P = 0.5$ μm, $h = 0.35$ μm, and $L = 1.0$. However, the interface profiles, which are determined by atomic force microscopy-based measurements, have been shown that the conformal growth of the layers does not occur in real solar cell structures. A $J_{\rm ph}$ of 16.2 mA/cm^2 has been achieved for a combination of $P = 0.5$ μm, $h = 0.35$, or 0.55 μm, and more realistic $L = 1.2$. One can expect that more pronounced gratings (larger h) result in a higher absorption level in both the "short" and "long" wavelength regions. However, in these cases, the losses occurring in the "long" wavelength region in the silver back reflector overshadow the increase of the absorption level within the a-Si:H layer. When the leveling L increases, an optimum period P shifts toward 0.25 μm.

D. μc-Si:H n-i-p Solar Cells

In this case, the thickness of the μc-Si:H absorber in the n-i-p solar cells has been fixed to 1.0 μm. The combinations of parameters $P = 0.5$–0.75 μm, $h = 0.55$ μm, and $L = 1.0$–1.1 result in $J_{\rm ph}$ 22.7–23 mA/cm^2. As mentioned in the previous section, a realistic degree of nonconformability of the structure is expected in the range $L = 1.2$–1.3. For this range of leveling, the maximal $J_{\rm ph}$ of 22.8 mA/cm^2 has been obtained for $P = 0.5$ μm, $h = 0.55$ μm, and $L = 1.2$. When the leveling increases, the front TCO layer becomes flatter, resulting in a larger total reflectance. With increasing h, an absorption of the μc-Si:H layer increases in both the "short" and "long" wavelength regions due to scattering and AR effects. Although the losses in the back reflector become also large, they do not mask the enhancement of the absorption.

E. Variation of the Silicon Absorber Thickness in p-i-n Solar Cells

The impact of the absorber thickness on the optimal geometrical parameters of the gratings has also been studied. For the a-Si:H p-i-n case, the absorber thickness $t_{\rm a\text{-}Si:H}$ has been varied from 0.1 to 0.3 μm. The optimal period P of the grating depends on the leveling L. In particular, when the leveling is small ($L = 1.1$), corresponding to almost conformal growth, the optimal period is affected by the thickness of a-Si:H layer. On the other hand, when $L = 1.3$ (moderate leveling), the optimal P has been found to be 0.6–0.75 μm and increases with the thickness. Larger values of h (0.25–0.45 μm in this case) result in larger absorption levels in all analyzed cases.

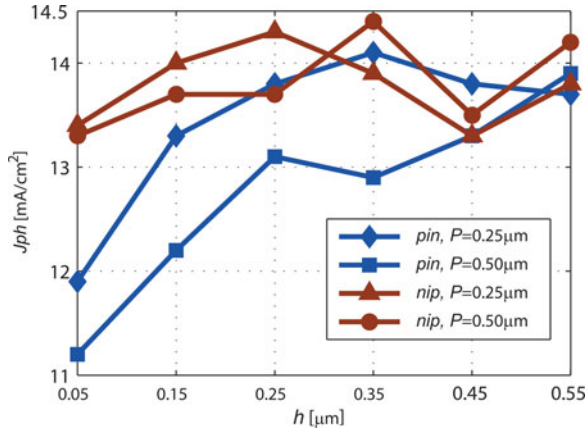

Fig. 5. $J_{\rm ph}$ for a-Si:H p-i-n and n-i-p solar cells generated under the "short" and "medium" wavelength illumination (0.35–0.66 μm) as a function of P and h with $d_C = 0.5$ and $L = 1.2$.

In μc-Si:H p-i-n solar cells, the thickness of the μc-Si:H absorber has been varied between 0.5 and 2 μm. For a moderate leveling $L = 1.3$, the optimal value of the period P has been found to be in the range 0.5–0.75 μm and increases with the thickness. When the leveling becomes smaller ($L < 1.2$), corresponding to a more conformal growth, the optimal value of P turns to be outside the simulation range. Furthermore, a larger height results in an enhanced absorption level for all considered absorber thickness values.

F. Antireflection Effect of the Gratings in the "Short" and "Medium" Wavelength Regions

The total reflection results in a significant loss of energy in thin-film silicon solar cells. SPG generally leads to a decrease of the total reflectance and, therefore, an increase of the amount of energy that is actually absorbed in a solar cell. The numerical simulations have shown that a substantial enhancement of the $J_{\rm ph}$ occurs in the "short" and "medium" wavelength ranges for smaller periods of the periodic grating. For a-Si:H solar cells, the AR effect of SPG with different P and h on $J_{\rm ph}$ is outlined in Fig. 5. SPG with a small P leads to an increase in $J_{\rm ph}$ regardless of the grating height value h in the p-i-n solar cells. For n-i-p configurations, the effect is not as clear as in the p-i-n ones, probably due to the smoothening that occurs during the deposition of the silicon layer. In general, increasing h results in an enhancement of $J_{\rm ph}$ in the "short" and "medium" wavelength ranges.

G. Light Trapping Effect in the "Long" Wavelength Region

Light trapping is essential for harvesting the "long" wavelength light inside solar cells. In a-Si:H solar cells, the selection of larger periods results in a larger $J_{\rm ph}$, especially in the n-i-p configuration. Increasing the height of the SPG also leads to an increase of $J_{\rm ph}$. In μc-Si:H n-i-p solar cells, larger periods also lead to a large $J_{\rm ph}$. Although increasing the height up to a certain value is beneficial in terms of $J_{\rm ph}$, the losses in (and near) metal back reflector increase as well and, hence, lower the gain.

TABLE III
MAXIMAL VALUES OF $J_{\rm ph}$ FOR p-i-n AND n-i-p a-Si:H AND μc-Si:H SOLAR CELLS WITH 1-D SPG AND WITH FLAT INTERFACES, ILLUMINATED WITH AM1.5G SPECTRUM, AND WAVELENGTH RANGE 350–1000 nm

Solar cell's structure and absorber material		P [μm]	h [μm]	L [-]	J_{ph} [mA/cm^2]	J_{ph} /$J_{ph,flat}$
a-Si:H *pin* ($t_{\text{a-Si:H}}$ = 0.3μm)	1-D	0.75	0.45	1.3	15.5	1.34
	flat	--	--	--	11.6	--
μc-Si:H *pin* ($t_{\text{μc-Si:H}}$ = 1μm)	1-D	0.50	0.45	1.3	20.3	1.24
	flat	--	--	--	16.4	--
a-Si:H *nip* ($t_{\text{a-Si:H}}$ = 0.3μm)	1-D	0.50	0.35-0.55	1.2	16.2	1.23
	flat	--	--	--	13.2	--
μc-Si:H *nip* ($t_{\text{μc-Si:H}}$ = 1μm)	1-D	0.50	0.45-0.55	1.1	23.0	1.38
	flat	--	--	--	16.7	--

In general, our analysis shows that gratings with larger periods are more efficient in trapping red and near infrared light.

H. Summary of the Results, $J_{\rm ph}$ Enhancement

We have carried out 2-D optical simulations in the wavelength range from 350 to 1000 nm for both p-i-n and n-i-p a-Si:H and μc-Si:H solar cells on SPG in order to determine potential $J_{\rm ph}$ for different parameters of the gratings. As a reference, we have computed the $J_{\rm ph.flat}$ of the same solar cell structures but with flat interfaces. The optimal set of grating parameters that results in the largest $J_{\rm ph}$ achieved in solar cells with SPG is reported in Table III. The $J_{\rm ph\text{-}flat}$ of the corresponding flat solar cell structures is also provided.

IV. CONCLUSION

A dedicated design methodology that is aimed at optimizing the thin-film silicon solar cells on 1-D SPG has been developed. The electric field distribution excited in different structures and resulting absorption in each layer were accurately calculated by solving Maxwell equations with FDTD method using the MEEP software package. The developed design tool has been validated by comparison with the ASA semiconductor device simulator, as well as the commercially available electromagnetic solvers CST Microwave Studio and Ansys HFSS.

The optimal parameters of the SPG that result in the maximum enhancement of the photocurrent density has been determined for both p-i-n and n-i-p a-Si:H and μc-Si:H single-junction solar cells. It was found that the effect of the nonconformal growth of the layers has a substantial influence on $J_{\rm ph}$. The enhancement in terms of $J_{\rm ph}$ relative to corresponding flat solar cells has been found to be 1.34 for a-Si:H p-i-n ($t_{\rm Si} = 0.3$ μm), 1.24 for μc-Si:H p-i-n ($t_{\rm Si} = 1$ μm), 1.23 for a-Si:H n-i-p ($t_{\rm Si} = 0.3$ μm), and 1.38 for μc-Si:H n-i-p ($t_{\rm Si} = 1$ μm). The optimal solar cell structures feature diffraction gratings with large aspect ratios. For such structures, the electric losses can be substantial. This can explain the discrepancy with the optimal values reported in the scientific literature.

The impact of the thickness t of the silicon absorbing layers (both a-Si:H and μc-Si:H) in p-i-n configuration on the optimal values of the period P and height h of the gratings has also been investigated. The study has shown that for variations of t ranging from 0.1 to 0.3 μm and with moderate leveling $L = 1.3$, the optimal values of P and h stay in the range 0.6–0.75 μm, $h \geq 0.45$ μm. For μc-Si:H p-i-n solar cells, the optimal value of P has been found to be in the range 0.5–0.75 μm, and it increases with the thickness.

The AR effect of SPG in the "short" and "medium" wavelength ranges and the light trapping properties in the "long" wavelength range for a-Si:H and μc-Si:H solar cells in both p-i-n and n-i-p configurations have been analyzed. When the period gets smaller, the reflectance in this wavelength range is decreased, thus enhancing the absorption of the structure. This effect results in an increase of $J_{\rm ph}$ but is unfortunately counter-balanced by a reduced scattering capability and, hence, a reduction $J_{\rm ph}$ in "long" wavelength range. It has been found that absorption losses in and close to the textured silver back reflector (back ZnO:Al/Ag interface) increase considerably with an increase of the height of the gratings.

The developed procedure can be used to accurately calculate absorption in each layer of thin-film silicon solar cells and to design the solar cell structure in order to maximize the photocurrent density.

ACKNOWLEDGMENT

The authors would like to thank J. Krč and R. Santbergen for fruitful discussions about solar cell modeling.

REFERENCES

[1] J. Bailat, L. Fesquet, J.-B. Orhan, B. Wolf, P. Madliger, J. Steinhauser, S. Benagli, D. Borrello, L. Castens, G. Monteduro, M. Marmelo, B. Dehbozorghi, E. Vallat-Sauvain, X. Multone, D. Romang, J.-F. Boucher, J. Meier, U. Kroll, M. Despeisse, G. Bugnon, C. Ballif, S. Marjanovic, G. Kohnke, N. Borrelli, K. Koch, J. Liu, R. Modavis, D. Thelen, S. Vallon, A. Zakharian, and D. Weidman, "Recent developments of high-efficiency micromorph tandem solar cells in KAI-M PECVD reactors," in *Proc. 25th Eur. Photovoltaic Solar Energy Conf.*, Valencia, Spain, 2008, pp. 2720–2723.

[2] M. Kambe, A. Takahashi, N. Taneda, K. Masumo, T. Oyama, and K. Sato, "Fabrication of A-Si:H solar cells on high haze SnO_2:F thin films," in *Proc. 33rd IEEE Photovoltaic Spec. Conf.*, San Diego, CA, 2008, pp. 1–4.

[3] O. Isabella, F. Moll, J. Krč, and M. Zeman, "Modulated surface textures using zinc-oxide films for solar cells application," *Phys. Status Solidi A*, vol. 207, pp. 642–646, 2010.

[4] J. Krč, M. Zeman, A. Čampa, F. Smole, and M. Topič, "Novel approaches of light management in thin-film silicon solar cells," in *Proc. Mater. Res. Soc. Symp.*, 2006, vol. 910, 0910-A25-01.

[5] F.-J. Haug, T. Söderström, O. Cubero, V. Terrazzoni-Daudrix, X. Niquille, S. Perregeaux, and C. Ballif, "Periodic textures for enhanced current in thin film silicon solar cells," in *Proc. Mater. Res. Soc. Symp.*, 2008, vol. 1101, 1101-KK13-01.

[6] Z. Yu, A. Raman, and S. Fan, "Fundamental limit of nanophotonic light trapping in solar cells," *Proc. Nat. Acad. Sci. U.S.A.*, vol. 107, pp. 17491–17496, 2010.

[7] F.-J. Haug, K. Söderström, A. Naqavi, and C. Ballif, "Resonances and absorption enhancement in thin film silicon solar cells with periodic interface texture," *J. Appl. Phys.*, vol. 109, pp. 084516-1–084516-8, 2011.

[8] C. Battaglia, C. M. Hsu, K. Söderström, J. Escarré, F. J. Haug, M. Charrière, M. Boccard, M. Despeisse, D. Alexander, and M. Cantoni, "Light trapping in solar cells: Can periodic beat random?," *ACS Nano*, vol. 6, pp. 2790–2797, 2012.

[9] O. Isabella, A. Čampa, M. Heijna, W. J. Soppe, R. van Erven, R. H. Franken, H. Borg, and M. Zeman, "Diffraction gratings for light trapping in thin-film silicon solar cells," in *Proc. 23rd Eur. Photovoltaic Solar Energy Conf.*, Valencia, Spain, 2008, pp. 2320–2324.

[10] T. Söderström, F.-J. Haug, X. Niquille, V. Terrazzoni, and C. Ballif, "Asymmetric intermediate reflector for tandem micromorph thin film silicon solar cells," *Appl. Phys. Lett.*, vol. 94, pp. 063501-1–063501-3, 2009.

[11] A. J. M. van Erven, J. Rutten, G. van der Hofstad, H. de Groot, M. Steltenpool, J. De Ruijter, B. Titulaer, H. Borg, and G. Rajeswaran, "Light-trapping enhancement by diffractive textures for thin-film silicon solar cells," in *Proc. 25th Eur. Photovoltaic Solar Energy Conf.*, Valencia, Spain, 2010, pp. 3181–3184.

[12] H. Sai, H. Fujiwara, and M. Kondo, "Back surface reflectors with periodic textures fabricated by self-ordering process for light trapping in thin-film microcrystalline silicon solar cells," *Solar Energy Mater. Solar Cells*, vol. 93, pp. 1087–1090, 2009.

[13] A. Čampa, O. Isabella, R. van Erven, P. Peeters, H. Borg, J. Krč, M. Topič, and M. Zeman, "Optimal design of periodic surface texture for thin-film a-Si:H solar cells," *Prog. Photovoltaics: Res. Appl.*, vol. 18, pp. 160–167, 2010.

[14] K. Söderström, F.-J. Haug, J. Escarré, O. Cubero, and C. Ballif, "Photocurrent increase in n-i-p thin film silicon solar cells by guided mode excitation via grating coupler," *Appl. Phys. Lett.*, vol. 96, pp. 213508-1–213508-3, 2010.

[15] D. Derkacs, S. Lim, P. Matheu, W. Mar, and E. Yu, "Improved performance of amorphous silicon solar cells via scattering from surface plasmon polaritons in nearby metallic nanoparticles," *Appl. Phys. Lett.*, vol. 89, no. 9, pp. 093103-1–093103-3, 2006.

[16] R. Dewan and D. Knipp, "Light trapping in thin-film silicon solar cells with integrated diffraction grating," *J. Appl. Phys.*, vol. 106, pp. 074901-1–074901-7, 2009.

[17] A. Čampa, O. Isabella, R. van Erven, P. Peeters, H. Borg, J. Krč, M. Topič, and M. Zeman, "Optimal design of periodic surface texture for thin-film a-Si:H solar cells," *Prog. Photovoltaics: Res. Appl.*, vol. 18, pp. 160–167, 2010.

[18] U. W. Paetzold, E. Moulin, B. E. Pieters, U. Rau, and R. Carius, "Optical simulations and prototyping of microcrystalline silicon solar cells with integrated plasmonic reflection grating back contacts," *Proc. SPIE*, vol. 8111, pp. 811107-1–811107-8, 2011.

[19] X. Sheng, S. G. Johnson, J. Michel, and L. C. Kimerling, "Optimization-based design of surface textures for thin-film Si solar cells," *Opt. Exp.*, vol. 19, no. S4, pp. A841–A850, 2011.

[20] O. Isabella, S. Solntsev, D. Caratelli, and M. Zeman, "3-D optical modeling of thin-film silicon solar cells on diffraction gratings," *Prog. Photovoltaics: Res. Appl.*, (Jan. 2012). [Online].

[21] S. Solntsev, O. Isabella, D. Caratelli, M. Kyriakou, O. Yarovyi, and M. Zeman, "Advanced optical modeling of thin-film silicon solar cells with 1-D periodic gratings," in *Proc. Mater. Res. Soc. Symp.*, 2011, vol. 1322, mrss11-1322-b08-19.

[22] S. Solntsev and M. Zeman, "Optical modeling of thin-film silicon solar cells with submicron periodic gratings and nonconformal layers," *Energy Procedia*, vol. 10, pp. 308–312, 2011.

[23] K. S. Yee, "Numerical solution of initial boundary value problems involving Maxwell's equations in isotropic media," *IEEE Trans. Antennas Propag.*, vol. AP-14, no. 3, pp. 302–307, May 1966.

[24] A. F. Oskooi, D. Roundy, M. Ibanescu, P. Bermel, J. D. Joannopoulos, and S. G. Johnson, "MEEP: A flexible free-software package for electromagnetic simulations by the FDTD method," *Comput. Phys. Commun.*, vol. 181, pp. 687–702, 2010.

[25] MATLAB environment. (2012). [Online]. Available: www.mathworks.nl/products/matlab

[26] O. Isabella, A. Čampa, M. Heijna, W. J. Soppe, R. van Erven, R. H. Franken, H. Borg, and M. Zeman, "Diffraction gratings for light trapping in thin-film silicon solar cells," in *Proc. 23rd Eur. Photovoltaic Solar Energy Conf.*, Valencia, Spain, 2008, pp. 2320–2324.

[27] Air Mass 1.5 AM1.5G spectra. (2012). [Online]. Available: http://rredc.nrel.gov/solar/spectra/am1.5

[28] CST—Computer Simulation Technology. (2012). [Online]. Available: www.cst.com/Content/Products/MWS/Overview.aspx

[29] Ansys HFSS official website. (2012). [Online]. Available: http://www.ansoft.com/products/hf/hfss

[30] M. Zeman and J. Krč, "Optical and electrical modeling of thin-film silicon solar cells," *J. Mater. Res.*, vol. 23, no. 4, pp. 889–898, Apr. 2008.

Authors' photographs and biographies not available at the time of publication.